# CHAPTER V

# EXPERIMENTAL RESULTS AND DISCUSSION II: ERBIUM-DOPED FIBER AMPLIFIER WITH OPTICAL CO-FEEDBACK

## 5.1 INTRODUCTION

In this chapter, the erbium-doped fiber amplifier (EDFA) system with optical co-feedback is presented. This scheme differs from the case of counter-feedback as presented in previous chapter in the direction of the optical isolator in the cavity. In such a scheme, the input signal and the oscillating laser are in the same direction. Comparison among the systems with co-feedback, counter-feedback and that without feedback is done in Sec. 5.3. Instead of saturation as exhibited in the counter-feedback scheme, the oscillating laser in the clock-wise direction in the co-feedback scheme effectively suppresses the backward amplified spontaneous emission (ASE). By varying the lasing wavelength, performance of the co-feedback scheme is compared with that of counter-feedback. The data is presented in Sec. 5.4. Both scheme manifested a noise behavior opposite to each other. Effects of the cavity loss on the amplifier performance as well as the oscillating laser will be described in Sec. 5.5. The oscillating laser itself subject to external injection is studied and is presented in Sec. 5.6.

## 5.2 EXPERIMENTAL SETUP

The configuration for demonstrating the EDFA with optical co-feedback is shown in Fig. 5.1. The system consists of two 980/1550 nm wavelength division multiplexers (WDMs), three couplers: $C_1$ and $C_2$, with an output coupling ratio of 95%, and $C_3$ for monitoring the spectrum in an anti-clockwise direction from the 1% port. A unidirectional oscillation of the laser was achieved using an isolator, ISO 1. Fig. 5.1 shows a **co-feedback** configuration where the laser oscillates in the direction of the input signal. It differs from the counter-feedback scheme as shown in Chapter 4 in the direction of the isolator. Without the tunable band-pass filter (TBF), the system is treated as a *regenerative EDFA* and will be demonstrated in next chapter. For the *system without optical feedback*, the ring was opened at the arm between ISO 1 and $C_3$. A-15-m long erbium-doped fiber (EDF) with a cutoff wavelength of 950 nm, a refractive index of 1.473 and an $Er^{3+}$ concentration of +440 ppm was used as an active medium. A 980 nm laser diode was used to pump the system from the 980 nm port of WDM I. The system was characterized at the signal wavelength of 1550 nm. The signal source was from an ANDO AQ4321D tunable laser source (TLS). The amplified output signal was monitored using an ANDO AQ6317B optical spectrum analyzer (OSA). The data presented in this chapter is referred to as *system value*. Time-Domain-Extinction (TDE) Method was applied in the system characterization.

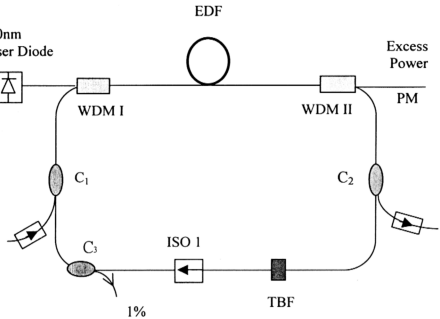


**Fig. 5.1** *Experimental setup for demonstrating the optical counter-feedback. (EDF: erbium-doped fiber; WDM: wavelength division multiplexer; C: coupler; ISO: isolator).*

## 5.3 AMPLIFIER PERFORMANCE – Comparison Among The Systems

### 5.3.1 Output Spectrums

Without input signal, the forward ASE output spectrum of the co-feedback scheme is compared with that of the systems with counter-feedback and that without feedback as shown in Fig. 5.2. The ASE spectrum closely emulates the gain spectral as will be discussed later. Thus, it provides useful information on the EDFA operating characteristics. The modes at the wavelength of ~1558 nm are the oscillating lasers in both co- and counter-feedback schemes. The systems were pumped at the maximum available power of 134.5 mW. A lower power level is exhibited in the systems with optical feedback since the population is clamped at the threshold after the onset of self-oscillation. Without the feedback, a much higher level of output power is observed.

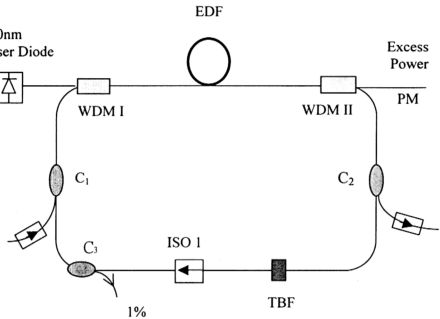


**Fig. 5.1** *Experimental setup for demonstrating the optical counter-feedback. (EDF: erbium-doped fiber; WDM: wavelength division multiplexer; C: coupler; ISO: isolator).*

## 5.3 AMPLIFIER PERFORMANCE – Comparison Among The Systems

### 5.3.1 Output Spectrums

Without input signal, the forward ASE output spectrum of the co-feedback scheme is compared with that of the systems with counter-feedback and that without feedback as shown in Fig. 5.2. The ASE spectrum closely emulates the gain spectral as will be discussed later. Thus, it provides useful information on the EDFA operating characteristics. The modes at the wavelength of ~1558 nm are the oscillating lasers in both co- and counter-feedback schemes. The systems were pumped at the maximum available power of 134.5 mW. A lower power level is exhibited in the systems with optical feedback since the population is clamped at the threshold after the onset of self-oscillation. Without the feedback, a much higher level of output power is observed.

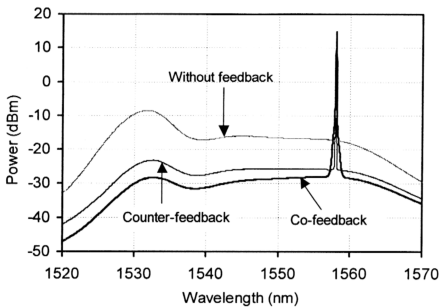


**Fig. 5.2** *Output spectrums without input signal at $P_p$ = 134.5 mW.*

### 5.3.2 Effects of Pump Power Variation

Signal gain as a function of pump power, $P_p$, with the input signal power fixed at $P_{in}$ = –31.2 dBm, for the systems with and without feedback is denoted in Fig. 5.3. After the onset of laser oscillation in the co- and counter-feedback systems at the threshold pump $P_{th}$ = 23.8 mW, signal gain becomes independent of the pump power since the population at the metastable level is clamped at threshold inversion. Note that the pump power, $P_p$, has been normalized to the threshold, $P_{th}$, as shown in in Fig. 5.3. All of the additional pumping power fed into this level then goes into the oscillating laser mode [1]. The gain compression of ~10 dB was observed at the

maximum available pump of 5.64 as compared to the system without optical feedback which has the maximum small-signal gain of 34 dB. For $P_p < P_{th}$, the effect of optical feedback is not obvious. All the systems manifest an identical signal gain and the simulation results match very well with the experimental data for low pump regime. The normalized pump power of $P_p = 0.5$ is the minimum pump power for bleaching the signal absorption, namely transparent pump power.

In a conventional EDFA, both signal gain and ASE power vary with the signal power and other parameters. In contrast, both signal gain and ASE power in the gain-clamped EDFA do not change significantly. Therefore, the noise figure is expected to change very little under different operation conditions. However, this assumption is not valid due to the existence of ASE self-saturation. Fig. 5.4 shows that the noise figure is increased by increasing the pump power for the scheme without feedback due to the self-saturation at the input end of the erbium-doped fiber caused by the increasing backward amplified spontaneous emission (ASE) with respect to the pump power. It is found that this effect is enhanced by introducing an optical feedback in the direction opposite that of the signal (counter-feedback). The noise figure for this feedback direction increased nearly linearly with the pump power and achieves its maximum value of 7.24 dB at the maximum available pump. Instead of the backward ASE, the degradation of the noise figure in this feedback scheme is mainly caused by the reduction of the population by the strong oscillating laser mode at the input end. Note that although the population is supposed to be clamped at its inversion after the onset of the laser oscillation, spectral hole burning, introduced by the strong oscillating laser, causes an incomplete clamping of the sub-levels [2]. Therefore, a slight variation of the population is expected due to the different levels of the laser strength. However, without considering the spectral hole burning effect, calculation in

Ref. [3] shows a decrease in the population inversion due to the saturation as the lasing power increases. An opposite behavior has been observed for the co-feedback scheme where the laser oscillated in the signal direction. It behaves like a counter-pumping configuration without optical feedback where the noise figure decreases with the pump power [4]. The discrepancy between simulation results and experimental data is consistent in this scheme. As shown in Fig. 5.4, the noise figure for this scheme reduces from 6.3 dB at the laser threshold to 5.6 dB at the maximum pump, which is 1.6 dB lower than that of the counter-feedback at the maximum pump. At the output end, stronger oscillating laser at the higher pump power suppresses the backward ASE generation, restoring the population to a higher level at the input end and resulting in a lower noise figure.

The PCE as a function of normalized pump power for different feedback schemes is denoted in Fig. 5.5. The input signal power used was $P_{in} = -31.2$ dBm. Without the optical feedback, the PCE increases to 1.45 % at the pump power of 82.4 mW and starts to saturate until the maximum available pump of 134.5 mW. Initially, the PCEs for both counter- and co-feedback schemes increase linearly, similar to that without feedback. It is worth noting that at the pump power of 23.8 mW, the PCEs for different feedback schemes start to depart from each other. The systems with counter- and co-feedback decrease from their maximum values of 0.67 % and 0.58 % at this pump power to 0.15 % and 0.12 %, respectively, at the maximum available pump. From the laser theory [1], it is stated that after the onset of the laser oscillation in the cavity, all of the additional pumping power fed into the metastable level then goes into the oscillating laser mode. Efficiency of power conversion to the input signal thus reduce after the threshold with the given input signal power. Consequently, the pump power that achieves the maximum PCE is the condition of the onset of laser

oscillation in the cavity with the feedback. Note that the counter-feedback scheme shows a slightly higher PCE as compared to the co-feedback scheme. Such a low PCE for both systems with optical feedback can be attributed to the small input signal power injected to the systems. PCE as high as 59% has been achieved with a heavily saturated input signal for the conventional configuration without feedback [5].

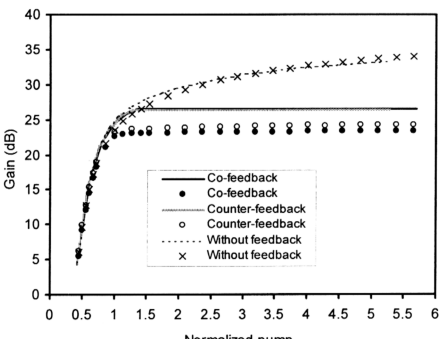


**Fig. 5.3** *Signal gain as a function of pump power with the input signal power fixed at $P_{in}$ = –31.2 dBm, for the systems with and without feedback. The pump power is normalized to the lasing threshold of 23.8 mW. (Point signs: Measured results; lines: Simulation results).*

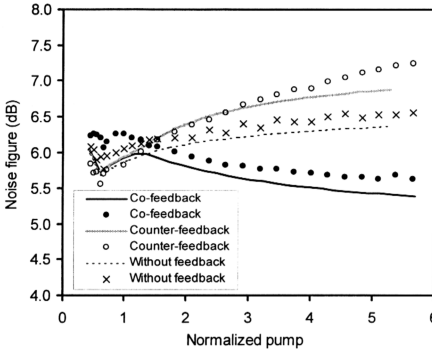


**Fig. 5.4** *Noise figure as a function of pump power with the input signal power fixed at $P_{in} = -31.2$ dBm, for the systems with and without feedback. The pump power is normalized to the lasing threshold of 23.8 mW. (Point signs: Measured results; lines: Simulation results).*

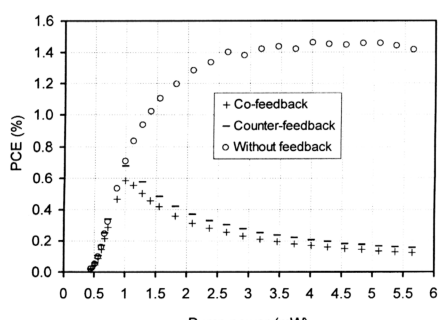


**Fig. 5.5** *PCE as a function of pump power with the input signal power fixed at $P_{in} = -31.2$ dBm, for the systems with and without feedback. The pump power is normalized to the lasing threshold of 23.8 mW.*

### 5.3.3 Effects of Input Signal Power Variation

Previous section concerns the EDFA system operated in the small-signal regime where the gain is independent of the input signal power $P_{in}$. In this section, the EDFA performance versus input signal power is addressed. Comparison is done for different feedback schemes. The experimental data together with the simulation results are demonstrated in Fig. 5.6. In this case, the pump power was fixed at the maximum normalized pump of 5.64. Gain saturation is reached when the EDFA characteristics depart from those linear relations. With the strong gain-clamping effect induced by the oscillating laser in the systems with optical feedback, linear amplification is preserved up to $P_{in} \approx$ -5 dBm. Fig. 5.6 shows that the saturation input power markedly increases from $P_{in}^{sat} = -19$ dBm for the system without feedback to –6 and –4.5 dBm for the counter-feedback and the co-feedback systems, respectively. However, this improvement is compensated at a cost of ~10 dB in gain compression. The maximum small-signal gain of 23.4 dB and 24.4 dB is achieved for the co- and counter-feedback schemes, respectively. These signal gains are relatively low as compared to the case without feedback since the inversion level has been clamped at the threshold $P_{th}$ = 23.8 mW. For the case without feedback, signal gain as high as 34.3 dB is achievable in the unsaturated regime.

The noise figure characteristics are shown in Fig. 5.7. Similar to the conventional co-pumping scheme [6], the system without optical feedback shows a dip in the saturated regime. In our case, the dip appears at the saturated input signal of –5 dBm. The dip effect arises from the suppression of the backward ASE by this high input signal power [6-8]. The existing strong backward ASE at the small input signal power causes ASE self-saturation at the input end, causing a higher noise figure in the unsaturated regime. Suppression of the backward ASE by a higher input power

restores the inversion to a higher level, thus, improving the noise figure by ~1 dB. The mechanism of such effect has been described in previous chapter. Generally, the decrease in noise figure is observed only in the system with high small-signal gain (i.e., G > 30 dB) [9]. However, with the counter-feedback scheme, the dip is striking although the small-signal gain of the system is just 24 dB. The depth of the dip in this case is 2.1 dB. Excluding the input coupling loss of 1.53 dB, noise figure as low as 3.21 dB has been achieved, showing a nearly complete suppression of the backward ASE. This is not the case for the co-feedback configuration where the noise figure is independent of input signal power until the maximum available input power of –2 dBm although the dip is still observed in the simulation. Note that in the unsaturated regime at this high pump power the backward ASE has already been suppressed by the oscillating laser in the clockwise direction. Therefore, the noise figure is much lower as compared to the rest of the feedback schemes, including the system without the optical feedback. With reference to the Fig. 5.6, it is found that the signal gain is 1 dB lower and saturation input signal power is 1.5 dB higher for co-feedback scheme than that of the counter-feedback scheme. This shows a stronger clamping effect of the former scheme. The oscillating laser is also supposed to suppress the backward ASE in this scheme, and resulting in increase of the population. However, the population tends to reduce to its inversion value at the threshold by reducing the absorption of the pump power due to the strong clamping effect, as given in Fig. 5.9.

With a lower normalized pump (1.8), thus, a weaker laser power, a dip with the depth of 0.2 dB for the co-feedback scheme is observed as shown in Fig. 5.8. With the weaker laser power in the clockwise direction, the noise figure is ~5.9 dB in the unsaturated regime, 0.3 dB higher than the case with the strong oscillating laser at the maximum power as shown in Fig. 5.7. A higher noise figure in the unsaturated regime

indicates a higher backward ASE at the higher pump power. Saturating signal with the power of –10 dBm is found to be able to suppress the arising backward ASE, leaving a dip with the depth of 0.2 dB. In the case of counter-feedback configuration the depth of dip increases to 1 dB at this pump power.

Fig. 5.9 shows the evidence of decrease in pump power absorption at the saturated input signal power in the case of co-feedback due to the strong clamping effect at the maximum available pump. The excess power increases by ~ 0.8 mW at the saturation input power $P_{in}^{sat}$ = -6 dBm. A striking feature of the data with the counter-feedback is that the excess pump is independent of the input signal power even in the saturated regime. As mentioned previously, nearly complete inversion is achieved in the input end in this case. Therefore, the amount of the absorbed pump power is expected to be lower. However, no significant variation of the excess power is observed. A plausible explanation is that the strong input signal created a signal-induced saturation along the EDF instead of the input end only. This cancels the effect of population variation throughout the fiber length. For the configuration without feedback, the population is not clamped. Increasing the input signal power would eventually increase the rate of depopulation along the fiber. More pump power would be absorbed due to the increase in the population at the ground state. As a result, excess power reduces accordingly.

Fig. 5.10 shows the amplified output signal power as a function of the input signal power for different feedback schemes at the maximum normalized pump power of 5.6. Due to the existence of the oscillating laser in the cavity in the systems with the optical feedback, linear amplification is possible for the input signal level up to the power of $P_{in}$ = -8 dBm before getting saturated. Without the feedback, linear amplification is only preserved for $P_{in}$ < -25 dBm. Basically, the inversion of the

amplifier with optical feedback is locked regardless of the amount of input signal power since the round-trip gain is clamped to be round trip loss at the lasing wavelength, provided enough pump power is available to keep the laser above threshold. However, limited by the maximum available pump power of 134.5 mW, the gain-clamping effect diminishes due to the gain quenching of the oscillating laser by the saturating input signal for $P_{in} > -5$ dBm. As a result, the systems with optical feedback behave like the system without feedback and the amplified output power for all the systems are identical.

In Fig. 5.11, the PCE for the systems operating from the unsaturated up to the moderately saturated input signal at the maximum normalized pump of 5.6 is presented. For the system without feedback, the PCE starts to increase nearly linearly after $P_{in} = -30$ dBm. The systems with the optical feedback show an exponentially increase only after $P_{in} = -20$ dBm. The highest discrepancy in the PCE among the systems occurs at $P_{in} = -5$ dBm. A striking feature is that the case shown in Fig. 5.5 is valid only for the unsaturated regime. Operating under the moderately saturated regime ($P_{in} \geq -6$ dBm), the PCE for the counter-feedback system starts to exceed that of the system without feedback with an amount of ~1.4 %. Under this saturation regime, the strong input signal starts to quench the gain of the oscillating laser and dominate the cavity. Due to the same reason, the PCE of the system with co-feedback is expected to approximate, if not exceed, the system without feedback in the heavily saturated regime.

amplifier with optical feedback is locked regardless of the amount of input signal power since the round-trip gain is clamped to be round trip loss at the lasing wavelength, provided enough pump power is available to keep the laser above threshold. However, limited by the maximum available pump power of 134.5 mW, the gain-clamping effect diminishes due to the gain quenching of the oscillating laser by the saturating input signal for $P_{in}$ > -5 dBm. As a result, the systems with optical feedback behave like the system without feedback and the amplified output power for all the systems are identical.

In Fig. 5.11, the PCE for the systems operating from the unsaturated up to the moderately saturated input signal at the maximum normalized pump of 5.6 is presented. For the system without feedback, the PCE starts to increase nearly linearly after $P_{in}$ = -30 dBm. The systems with the optical feedback show an exponentially increase only after $P_{in}$ = -20 dBm. The highest discrepancy in the PCE among the systems occurs at $P_{in}$ = –5 dBm. A striking feature is that the case shown in Fig. 5.5 is valid only for the unsaturated regime. Operating under the moderately saturated regime ($P_{in} \geq$ -6 dBm), the PCE for the counter-feedback system starts to exceed that of the system without feedback with an amount of ~1.4 %. Under this saturation regime, the strong input signal starts to quench the gain of the oscillating laser and dominate the cavity. Due to the same reason, the PCE of the system with co-feedback is expected to approximate, if not exceed, the system without feedback in the heavily saturated regime.

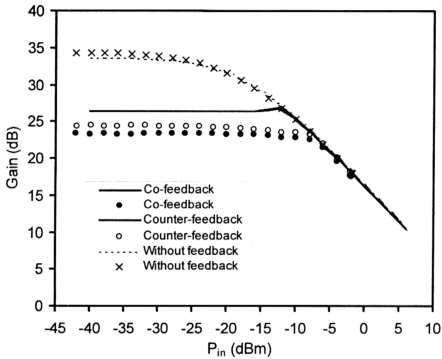


**Fig. 5.6** *Signal gain as a function of input signal power at the maximum normalized pump power of 5.6. (Point signs: Measured results; lines: Simulation results).*

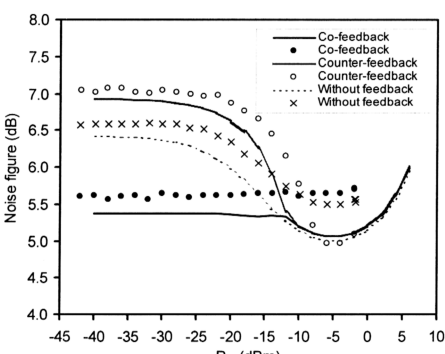


**Fig. 5.7** *Noise figure versus input signal power at the maximum normalized pump power of 5.6. (Point signs: Measured results; lines: Simulation results).*

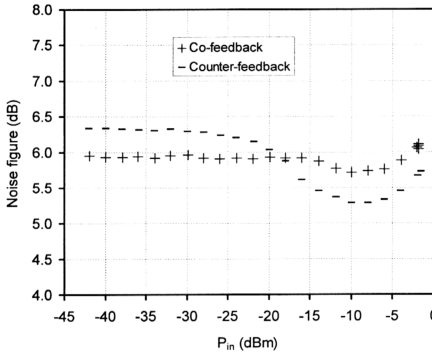


**Fig. 5.8** *Noise figure versus input signal power at the normalized pump power of 1.8.*

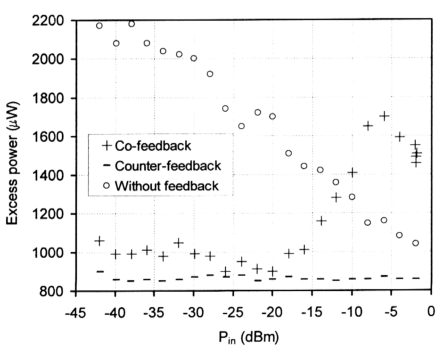


**Fig. 5.9** *Excess pump power as a function of input signal power for different feedback schemes at the maximum pump power.*

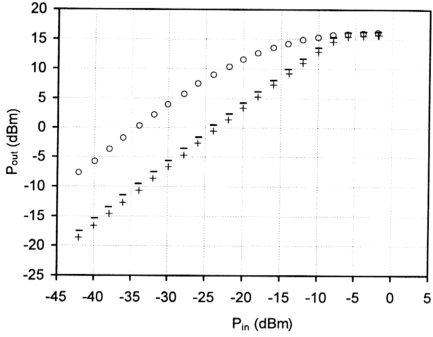


**Fig. 5.10** *Amplified output signal power as a function of input signal power. (+: co-feedback; -: counter-feedback; o: without feedback).*

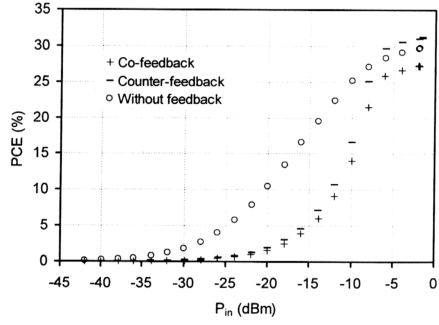


**Fig. 5.11** *PCE for the systems operating from unsaturated up to moderately saturated input signal at the maximum normalized pump of 5.6*

### 5.3.4 Effects of Signal Wavelength Variation

The gain spectral for different feedback schemes at the maximum pump power is illustrated in Fig. 5.12. It closely emulates the ASE power spectrum. The signal gain for the system without feedback is much higher since laser oscillation does not take place. Signal gain as high as 39.1 dB is achieved in this system at $\lambda_{sig}$ = 1532 nm. A fairly flat gain can be obtained in the wavelength range of 1540 nm to 1560 nm with an average gain of 34 dB. With the optical feedbacks, the inversion is clamped at a lower level, resulting in a low signal gain over the entire amplification bandwidth. The existence of the oscillating laser in these systems modifies the spectral distribution of the photons through saturation and multiphonon transition. Saturation takes place mainly in the high gain wavelength regime around 1533 nm. This increases the photons absorption at 1560 nm wavelength region. Multiphonon transition then shifts the population to the larger wavelength region centered at this wavelength region in the systems with optical feedbacks. Maximum gain of 24.9 dB is achieved in the counter-feedback scheme whereas the co-feedback scheme achieves the gain by 0.8 dB lower.

Noise figure as a function of signal wavelength at the maximum pump power is denoted in Fig. 5.13. Note that the noise figure for the system with co-feedback is among the lowest. In Fig. 5.12, it is shown that the signal gain for the system with counter-feedback is slightly higher as compared to that with co-feedback. This shows that the former has an average inversion level higher than that of the latter case. However, the noise figure for the former case is among the highest as shown in Fig. 5.13. This is due to the lower inversion level at the EDF input end. It has been shown that the noise figure for an EDFA system is dependent on the inversion level at this EDF portion [3, 9]. With the co-feedback configuration, the backward ASE at the

EDF input end is effectively suppressed by both input signal and oscillating laser. Therefore, a higher inversion level is achievable. Instead of the backward ASE suppression, the strong oscillating laser in the anti-clockwise direction in the counter-feedback scheme induces saturation at the EDF input end, thus, giving a much higher noise figure. The higher noise figure at the short wavelength region can be attributed to the smaller spontaneous emission factor, $n_{sp}$ in this wavelength region as given by Eq. (2.30).

Fig 5.14 shows the power conversion efficiency, PCE, as a function of signal wavelength, $\lambda_{sig}$ at the maximum pump power. The input signal power was fixed at $P_{in}$ = -32.1 dBm. Right-hand-side axis is used to provide a clearer indication of the values for the systems with optical feedback due to the low value of the PCE. Note that the PCE curves for all the schemes follow the gain spectral and ASE spectrum since the PCE is gain dependent. Therefore, there are two PCE peaks centered at $\lambda_{sig}$ = 1533 nm and $\lambda_{sig}$ = 1558 nm. Maximum PCE of 4.5% is achieved at $\lambda_{sig}$ = 1533 nm for the system without feedback. For the systems with the co- and counter-feedback, the maximum PCE is achieved at $\lambda_{sig}$ = 1558 nm rather than at $\lambda_{sig}$ = 1533 nm due to the multiphonon transition that shifts the gain toward longer wavelengths. Maximum PCEs achieved in the co- and counter-feedback schemes are 0.18 % and 0.14 %, respectively.

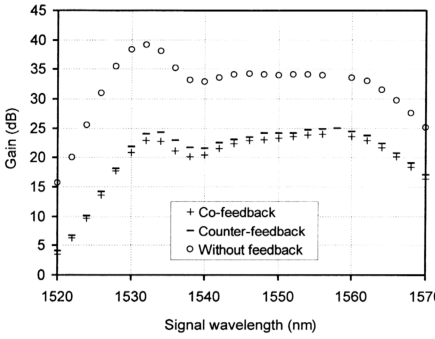


**Fig. 5.12** *Signal gain as a function of signal wavelength at the pump power $P_p$ = 134.5 mW.*

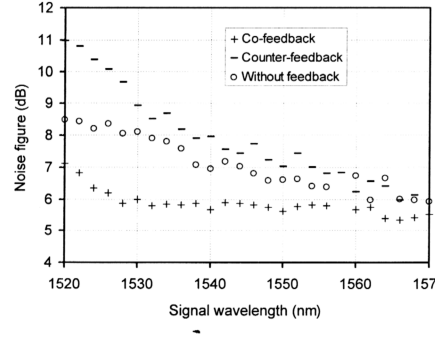


**Fig. 5.13** *Noise figure as a function of signal wavelength at the pump power $P_p$ = 134.5 mW.*

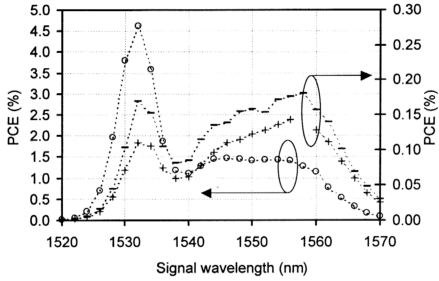


**Fig. 5.14** *PCE as a function of signal wavelength at the pump power of 134.5 mW. (+: co-feedback; -: counter-feedback; o: without feedback)*

## 5.4 VARIATION OF LASING WAVELENGTH

The lasing wavelength is tuned for every 2 nm step ranging from 1525 nm to 1565 nm. The signal gain at the wavelength of $\lambda_{sig}$ = 1550 nm as a function of the oscillating lasing wavelength, $\lambda_{laser}$, for both counter- and co-feedback schemes, is shown in Fig. 5.15. The counter-feedback scheme shows a higher signal gain over the entire amplification bandwidth. Within the tuning range of the TBF, there were three maximum signal gains at $\lambda_{laser}$ = 1525, 1539, and 1564 nm and two minimum at 1533 and 1558 nm. Redistribution of the photon statistic over the emission spectrum occurs when the oscillating laser is tuned over the entire amplification bandwidth. A striking feature is that the plots show an inverse relation with the forward ASE output spectrum from an under-pumped EDF (see Fig. 5.16). In the ASE spectrum, there are two gain peaks centered at the wavelengths of 1533 and 1558 nm. As a result, the injected signal at the wavelength of 1550 nm experiences more gain quenching effect

when the laser is tuned to these two wavelengths. Fig. 5.15 shows that the signal gains are 25.7 dB and 23.5 dB for $\lambda_{laser}$ = 1533 and 1558 nm, respectively, for the co-feedback scheme. For the counter-feedback scheme, the corresponding signal gains are 26.6 dB and 24.3 dB, respectively. Note that the gain quenching effect is not only dependent on the ASE spectrum, but also the wavelength separation between the oscillating laser and the injected signal. Although the gain peak is high at the wavelength of 1533 nm in the ASE spectrum, the gain quenching effect is less as compared to the case when the lasing wavelength is tuned to the region near the injected signal around 1558 nm. At the wavelength of 1525 nm, the laser strength is weaker due to the lower population at the corresponding sublevels. This enables a higher population at the wavelength region around 1550 nm, resulting in a maximum signal gain of ~33 dB for both feedback schemes. Moreover, lasing wavelength of 1525 nm is far from the injected signal wavelength of 1550 nm. Consequently, gain-quenching effect is less. For the lasing wavelength of 1539 nm, there is a gain peak for each feedback scheme. This wavelength is corresponding to the dip in the ASE spectrum. A higher population is obtained at the region around the wavelength of 1550 nm when the oscillating laser is tuned to the dip.

The variation in signal gain with respect to the lasing wavelengths corresponds to the power level variation of the output ASE spectrum at the 1550 nm region as shown in Fig. 5.16. The output spectrums for both counter-feedback (dashed line) and co-feedback (solid line) without the probe signal are presented at $\lambda_{laser}$ = 1525, 1533, 1539, and 1558 nm. At $\lambda_{laser}$ = 1525 nm, the signal at 1550 nm shows the highest signal gain. This is attributed to the weak oscillation at this wavelength that allows a high population at the 1550 nm region. The corresponding ASE level at 1550 nm as shown in Fig. 5.16(a) is –17.8 dBm. Note that for the counter-feedback, the oscillating

laser was supposed to be eliminated at the output port. However, the back-reflected laser still exists at the output port due to the reflection from the terminated port of the couplers and the splicing mismatch between the EDF and the Flexcor fiber used in the WDM couplers. When the laser is tuned to 1533 nm where it experiences a strong amplification, the ASE level at the 1550 nm region (Fig. 5.16(b)) reduces to -26.5 dBm. This results in the signal gain reduction. At 1539 nm, which is corresponding to the dip region of the ASE spectrum as shown in Fig. 5.16(c), the laser strength is reduced. The population is now higher at 1550 nm, resulting in a higher signal gain. By tuning the laser to the wavelength of $\lambda_{laser}$ = 1558 nm, the minimum signal gain is achieved due to the high depletion rate of the population at the 1550 nm region where the spectrum level suppression of 4.4 dB is observed as compared to the case when the laser is fixed at $\lambda_{laser}$ = 1539 nm. The corresponding gain reduction is 4.3 dB. Note that the entire ASE level is suppressed, as shown in Fig. 5.16(d), when the laser is tuned to $\lambda_{laser}$ = 1558 nm.

Fig. 5.17 shows dependence of the noise figure on the lasing wavelength which induces the population variation for both counter- and co-feedback schemes. The most important feature of these measurements is the opposite behavior between both feedback schemes. Let us consider first the case of the counter-feedback. At $\lambda_{laser}$ = 1525 nm, the ASE spectrum (as shown in Fig. 5.16(a)) is high at the 1550 nm region due to the weaker laser power. The higher ASE spectrum from the output end in such a co-pumping scheme signify a high population. Therefore, a lower noise figure (6.7 dB) is achieved with this lasing wavelength. The population decreases at the 1550 nm region as the laser is tuned to the wavelengths such as 1533 and 1558 nm. As shown in Fig. 5.16(b) and (d), the entire ASE spectrum has been suppressed with these lasing wavelengths and the noise figures are 6.9 and 7.4 dB, respectively.

For the co-feedback system, the noise figure shows a totally different behavior opposite that of the counter-feedback system. The data is illustrated in Fig. 5.17. At the lasing wavelength of $\lambda_{laser}$ = 1525, 1539 and 1564 nm in co-feedback scheme, the population is supposed to be higher due to the smaller gain quenching effect. Therefore, the noise figure is expected to be lower. However, the noise figure shows a behavior opposite to what is expected. Instead of population variation due to the laser power variation as in the case of counter-feedback, the laser entering the input end of the active medium in the co-feedback system plays an important role of backward ASE suppression at this end [8]. This backward ASE causes the population depletion or ASE self-saturation at this fiber portion, thus, resulting in a higher noise figure. The strong oscillating laser at the wavelengths of $\lambda_{laser}$ = 1533 nm and $\lambda_{laser}$ = 1558 nm efficiently suppresses the backward ASE, restoring the population to a higher level. A higher ASE spectrum level in these two cases is attributed to the contribution from the forward ASE coming out from the output port. Excluding the input coupling loss of 1.53 dB, noise figure as low as 3.84 dB has been achieved for the signal wavelength of 1550 nm at the lasing wavelength of 1533 nm, showing a high inversion of the erbium ions in this case.

With the smaller pump power of 43.4 mW, 1.8 times above the oscillation threshold, the laser induced saturation in the counter-feedback scheme and the backward ASE suppression by the oscillating laser in the co-feedback scheme become insignificant. Therefore, the noise figures are almost identical for both feedback schemes. The data is illustrated in Fig. 5.18. The oscillating laser is relatively weak at this pump power as compared to the previous case. In the case of counter-feedback, the noise figure is markedly improved and it is < 6.3 dB over the entire tuning range of the oscillating laser. The saturation effect at the EDF input end is less as compared

to the case when $P_p$ = 134.5 mW. However, in the case of the co-feedback at this low pump power, the backward ASE is not effectively suppressed by the weaker oscillating laser in the clockwise direction. The noise figure is thus degraded by ~0.5 dB.

The oscillation threshold of the laser itself is studied as a function of laser tuning wavelength for the co-feedback scheme. The data is depicted in Fig. 5.19. The curve exhibits an inverse relation with the ASE output profile. At the wavelength of 1525 nm when the gain is low, the pump power as high as $P_{th}$ = 100.3 mW is required to achieve the condition of the laser oscillation. Since the threshold is high, the population is clamped at a higher inversion. Therefore, with the input signal injected at $\lambda_{sig}$ = 1550 nm as shown in Fig. 5.15, a higher signal gain is achievable. In the high gain regime around 1533 nm, the threshold is the lowest, i.e., $P_{th}$ = 25.1 mW. Therefore, the population is clamped at a lower inversion level. Such a low threshold allows the oscillating laser to build up to a higher level since all the addition pump power feedback into the metastable level will go into the oscillating mode [1].

Fig. 5.20 shows the power conversion efficiency, PCE, as a function of lasing wavelength. The data shows an inverse relation with the ASE spectrum and the curve-shape is similar to the gain curve as shown in Fig. 5.15. With the strong oscillating laser at $\lambda_{laser}$ = 1533 nm and 1558 nm, the signal at $\lambda_{sig}$ = 1550 nm experiences the lowest gain, thus the lowest PCE. When the laser is tuned to the wavelength region where the gain is lower such as $\lambda_{laser}$ = 1525 nm, 1539 nm and 1564 nm, the oscillating laser is relatively weak. The saturation effect is less especially at the lasing wavelength of 1525 nm. Therefore, the population is high at the sublevels corresponding to the wavelength of 1550 nm. As a result, PCE as high as 1.17 % and 1.21 % can be achieved for the co- and counter-feedback scheme, respectively.

PERPUSTAKAAN UNIVERSITI MALAYA

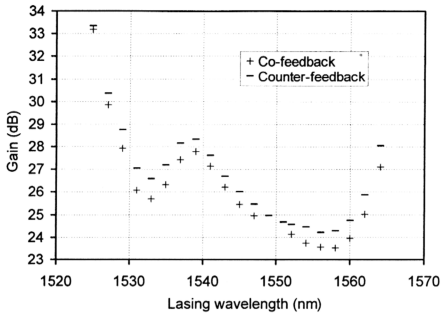


**Fig. 5.15** *Signal gain at $\lambda_{sig}$ = 1550 nm as a function of the oscillating lasing wavelength for both counter- and co-feedback schemes.*

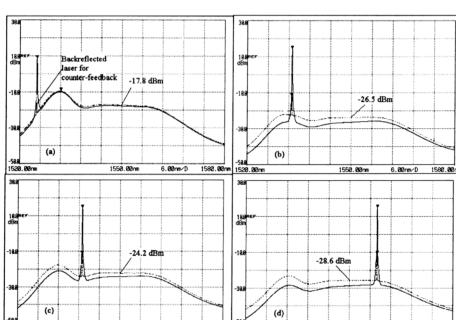


**Fig. 5.16** *ASE spectrums for co-feedback (solid line) and counter-feedback (dashed line). (a). $\lambda_{sig}$ = 1525 nm, (b). $\lambda_{sig}$ = 1533 nm, (c). $\lambda_{sig}$ = 1539 nm and (d). $\lambda_{sig}$ = 1558 nm.*

PERPUSTAKAAN UNIVERSITI MALAYA

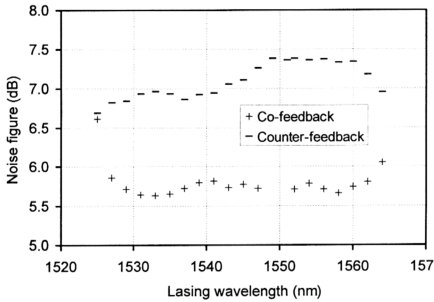


**Fig. 5.17** *Dependence of the noise figure on the lasing wavelength for both counter- and co-feedback schemes at $P_p$ = 134.5 mW.*

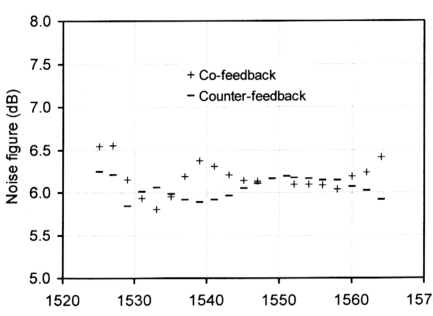


**Fig. 5.18** *Dependence of the noise figure on the lasing wavelength for both counter- and co-feedback schemes at $P_p$ = 43.4 mW.*

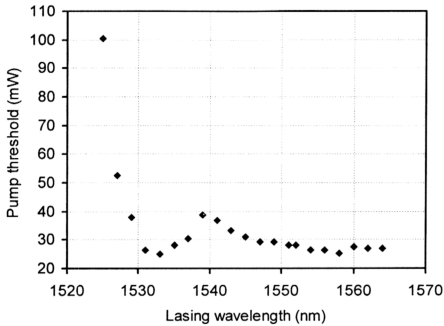


**Fig. 5.19** *Oscillation threshold of the laser as a function of tuning wavelength.*

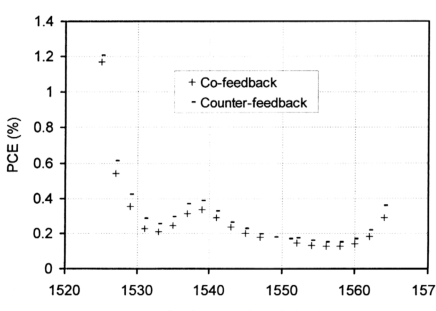


**Fig. 5.20** *PCE as a function of lasing wavelength at $P_p$ = 134.5 mW.*

## 5.5 STUDY OF CAVITY LOSS

In this study, cavity loss of the co-feedback scheme is controlled by varying the attenuation of a variable optical attenuator (VOA) placed in the cavity between isolator and coupler $C_3$ as shown in Fig. 5.1. The insertion loss of ~2.5 dB is introduced to the cavity although the attenuation is tuned to be 0 dB. The oscillating laser was arbitrarily fixed at $\lambda_{sig}$ = 1539 nm. Peak power of the oscillating laser is studied as a function of VOA attenuation. The data is denoted in Fig. 5.21. With the moderate attenuation, the laser peak power starts to decrease steeply from the attenuation of 3 dB for $P_p$ = 89 mW and 4 dB for $P_p$ = 103.5 mW. A higher attenuation forces the system to operate below the threshold of self-oscillation. The laser peak power < 0 dBm is basically considered as below oscillation threshold since the signal-to-noise ratio, $SNR_{(laser)}$ is < 20 dB.

Fig. 5.22 shows the dependence of the signal gain on the VOA attenuation for $P_p$ = 89 mW and 134.5 mW. The input signal was injected at $\lambda_{sig}$ = 1550 nm and at $P_{in}$ = -31.2 dBm. At low attenuation, the signal gain increases linearly with the cavity loss. This is attributed to the decrease in the level of the oscillating laser with the cavity attenuation. Therefore, the threshold inversion is increased to a higher level and thus, a higher signal gain is achievable. With the pump power of $P_p$ = 89 mW, the gain increases linearly until the attenuation of 4 dB after which the gain becomes independent of the attenuation. The phenomenon is corresponding to the situation where the gain-clamping effect is no longer preserved. The system is now operating below the oscillation threshold, similar to the conventional EDFA without feedback. A constant gain of 32.7 dB is obtained at this pump power. With a higher pump power of $P_p$ = 134.5 mW, the gain-clamping effect is stronger. Consequently, a higher attenuation level is required to suppress the oscillating laser. Fig. 5.22 shows that the

signal gain becomes constant after the attenuation of 6 dB. In this case, the constant gain is 34.4 dB.

The output spectrum for different attenuation level at $P_p$ = 134.5 mW is illustrated in Fig. 5.23. A small signal of $P_{in}$ = -31.2 dBm was injected at $\lambda_{sig}$ = 1550 nm. With the attenuation of 2 dB as shown in Fig. 5.23(a), the oscillating laser at $\lambda_{laser}$ = 1539 nm achieves a peak power as high as 12.3 dBm. Increasing the attenuation by another 2 dB decreases the laser peak power to 8.8 dBm as depicted in Fig. 5.23(b). The system is forced to operate below the oscillation threshold when the attenuation increases to 6 dB and 8 dB, as shown in Fig. 5.23(c) and 5.23(d), respectively. It is worth noting that the power level of the spectrum increases with the attenuation level. As a result, the signal at $\lambda_{sig}$ = 1550 nm experiences a higher amplification. However, after elimination of the gain clamping effect, the power level remains unchanged and the gain becomes independent of the attenuation level, consistent with the data illustrated in Fig. 5.22.

The dependence of the noise figure on the VOA attenuation is shown in Fig. 5.24. As mentioned earlier, increasing the cavity loss will eventually increase the average inversion of the active medium and thus the signal gain. However, increase in the average inversion does not decrease the noise figure as it should be. This can be attributed to the low inversion level at the EDF input end. With the small input signal of $P_{in}$ = -31.2 dBm and the small cavity loss, strong oscillating laser in the clockwise direction effectively suppresses the backward ASE at the EDF input end and prevents the backward ASE from generating from the EDF output end. Therefore, with the strong oscillating laser at the small cavity loss, the inversion level at the EDF input end is higher, resulting in a lower noise figure. Efficiency of the backward ASE suppression decreases with cavity loss due to the decrease in the level of the

oscillating laser. Under the condition of unclamping where the system operates below the oscillation threshold, the inversion level at the EDF input end basically remains unchanged although the cavity loss is increased without changing other parameters. This is observed after the attenuation level of 4 dB for $P_p$ = 89 mW and 6 dB for $P_p$ = 134.5 mW where the noise figure fixed at the values of 5.6 dB and 5.7 dB, respectively. In Fig. 5.23(c) and (d), the power level of the spectrum is identical under the unclamped condition. The power level is basically contributed by the single-pass forward ASE which is independent of the cavity loss.

Without the input signal, the oscillation threshold is studied as a function of the VOA attenuation. We define the oscillation threshold in this case to be $(SNR)_{laser} \geq 20$ dB. In laser system, the round-trip gain should be equal to the cavity loss in order to achieve the condition of laser oscillation [1, 10]. By increasing the cavity loss, a higher gain, produced by a higher pump power, is required to achieve the threshold condition. In consequence, the oscillation threshold increases with the VOA attenuation as illustrated in Fig. 5.25. With the lasing wavelength fixed at $\lambda_{laser}$ = 1539 nm, the threshold pump power for the zero attenuation level is determined to be 53.1 mW. It increases exponentially with the VOA attenuation. With the maximum achievable pump power of $P_p$ = 134.5 mW, laser oscillation cannot be sustained beyond the attenuation level of 5.4 dB.

With the signal injected at $\lambda_{sig}$ = 1550 nm and at $P_{in}$ = -31.2 dBm, power conversion efficiency is studied as a function of VOA attenuation as denoted in Fig. 5.26. The PCE increases linearly with the cavity loss under the condition of gain clamping. At the higher attenuation level when the gain clamping effect is no longer preserved, the PCE becomes constant. Both pump powers of $P_p$ = 89 mW and 134.5 mW exhibit amost identical PCE (~1.6 %) due to the signal-induced saturation.

In Fig. 5.27, amplified output signal power, $P_{out}$, at $\lambda_{sig}$ = 1550 nm as a function of laser peak power, $P_{laser}$ is illustrated. With the fixed pump powers of $P_p$ = 89 mW and 134.5 mW, the laser power is varied by varying the VOA attenuation. As mentioned earlier, the laser power < 0 dBm is basically not considered as a laser since $(SNR)_{laser}$ < 20 dB as shown in Fig. 5.23(c). Therefore, variation of the $P_{laser}$ in this regime will not affect the inversion level. Fig. 5.27 shows that $P_{out}$ exhibits a constant value of 1.5 dBm and 3.2 dBm for $P_p$ = 89 mW and 134.5 mW, respectively. Above the oscillation threshold where $P_{laser}$ > 0 dBm and $SNR_{(laser)}$ > 20 dB, the $P_{out}$ starts to be dependent on the $P_{laser}$.

Similar curve is obtained for the plot of gain versus laser power as shown in Fig. 5.28. Under the unclamping condition, constant gains of 32.6 dB and 34.3 dB are exhibited for $P_p$ = 89 mW and 134.5 mW. With the existence of the laser oscillation, the signal gain is quenched and decreased by the oscillating laser. A large data variation for the case of $P_p$ = 134.5 mW at the high $P_{laser}$ is attributed to the instability in the laser peak power due to the mode competition arising from the inhomogenity in the active medium. In next section, improvement of the laser stability with an external injection will be described.

Fig. 5.29 shows the dependence of the noise figure on the laser power, $P_{laser}$ with the fixed pump powers of $P_p$ = 89 mW and 134.5 mW. With the existence of the oscillating laser ($P_{laser}$ > 0 dBm), the noise figure is dependent on the laser power. A striking feature is that although the strong oscillating laser quenches the gain of the active medium and thus the average inversion level, the noise figure is not degraded. Instead of degradation, the noise figure decreases with the laser power due to the backward ASE suppression by the oscillating laser in the clockwise direction.

Power conversion efficiency, PCE, as a function of the laser peak power, $P_{laser}$, is shown in Fig. 5.30. The PCE (~1.6 %) is independent of the laser power under the unclamped condition since the pump power and the input signal are fixed. The decrease in the PCE with the laser power above the oscillation threshold is due to the decrease in the amplified output signal power as given by Eq. 4.1, as a result of the gain quenching induced by the strong oscillating laser.

With the pump fixed at the maximum available power of $P_p$ = 134.5 mW, the signal gain is studied as a function of the input signal power, $P_{in}$, for different attenuation level of 0 dB, 3 dB and 6 dB. The data is illustrated in Fig. 5.31. Without the gain-clamping effect when the attenuation level is 6 dB, the amplifier system saturates at $P_{in}^{sat}$ = -20 dBm with the small-signal gain of 34.5 dB. With the existence of the oscillating laser in the cavity at the attenuation levels of 3 dB and 0 dB, the saturation input powers are increased to $P_{in}^{sat}$ = –16 dBm and –15 dBm, respectively. However, the small-signal gain is compressed to 32.4 dB and 30.3 dB, respectively.

The dependence of the noise figure on the input signal power is denoted in Fig. 5.32. At the attenuation level of 6 dB, the amplifier system is operating below the oscillation threshold. The high noise figure (~5.9 dB) in the small signal regime indicates a strong backward ASE existing at the EDF input portion. Such a backward ASE can be suppressed by increasing the $P_{in}$. A dip at $P_{in}$ = -10 dBm reveals that the backward ASE is effectively suppressed, resulting in a higher inversion level at the EDF input end. With the existence of the oscillating laser at the attenuation levels of 3 dB and 0 dB, the backward ASE can be suppressed although the input signal is small. The lowest noise figure (5 dB) is achievable when the laser level is the highest, indicating a nearly complete suppression of backward ASE. In this case, it is worth noting that the noise figure increases slightly at $P_{in}$ = -16 dBm. At this input signal

level, the gain of the oscillating laser is quenched and the system operates below the oscillation threshold. The mechanism of the backward ASE suppression partially diminishes since $P_{in}$ = -16 dBm is not the optimum signal level to suppress the backward ASE at the given pump powers. By increasing the $P_{in}$ to –10 dBm, the backward ASE is effectively suppressed. Above $P_{in}$ > -10 dBm, signal-induced saturation starts to come into play and the noise figure starts to increase progressively.

Fig. 5.33 shows the power conversion efficiency, PCE, as a function of the input signal power, $P_{in}$. In the small-signal regime, the discrepancy among different attenuation levels cannot be seen clearly. It can only be differentiated at the input signal around –25 dBm. With the strongest oscillating laser existing in the cavity at the attenuation level of 0 dB, the PCE is among the lowest. All of the pump power provided to the amplifier system is converted into the oscillating mode. The highest PCE is achieved when the system is operating below the threshold of self-oscillation at the attenuation level of 6 dB. Above $P_{in}$ > -15 dBm, the oscillating laser is quenched. Thus, the system behaves like a conventional amplifier system without feedback, regardless of the attenuation level and the PCEs become identical with the maximum PCE of 28.6 %.

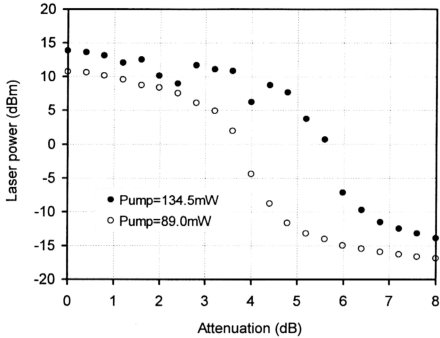


**Fig. 5.21** *Peak power of the oscillating laser as a function of VOA attenuation for $P_p$ = 89 mW and 134.5 mW.*

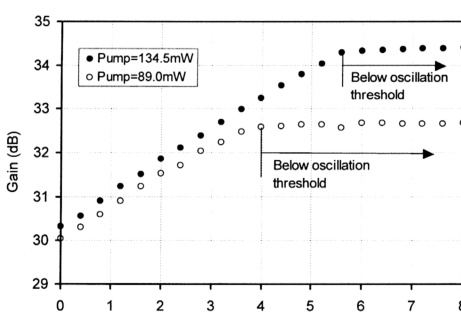


**Fig. 5.22** *Dependence of the signal gain on the VOA attenuation for $P_p$ = 89 mW and 134.5 mW.*

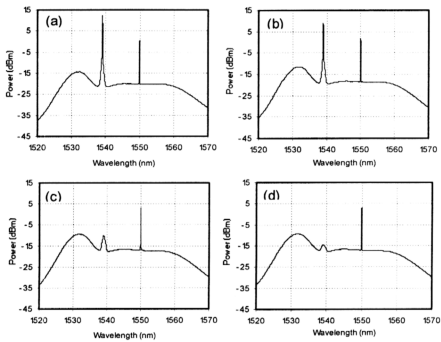


**Fig. 5.23** *Output spectrum for different attenuation level of (a). 2 dB, (b). 4 dB, (c). 6 dB and (d). 8 dB at $P_p$ = 134.5 mW. A small signal of $P_{in}$ = -31.2 dBm is injected at $\lambda_{sig}$ = 1550 nm.*

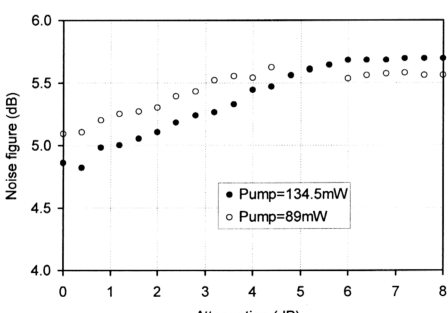


**Fig. 5.24** *Dependence of the noise figure on the VOA attenuation at $P_p$ = 134.5 mW. A small signal of $P_{in}$ = -31.2 dBm is injected at $\lambda_{sig}$ = 1550 nm.*

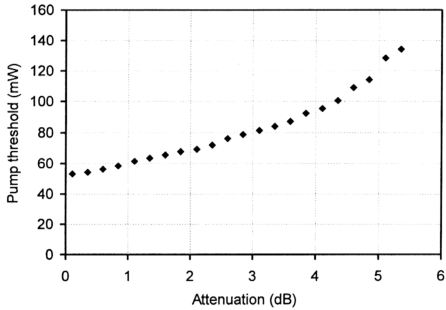


**Fig. 5.25** *Oscillation threshold as a function of attenuation level.*

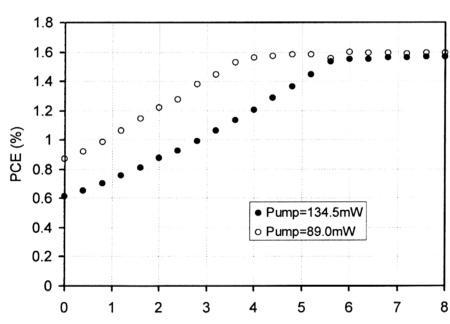


**Fig. 5.26** *Power conversion efficiency as a function of VOA attenuation with the signal injected at $\lambda_{sig}$ = 1550 nm and at $P_{in}$ = -31.2 dBm.*

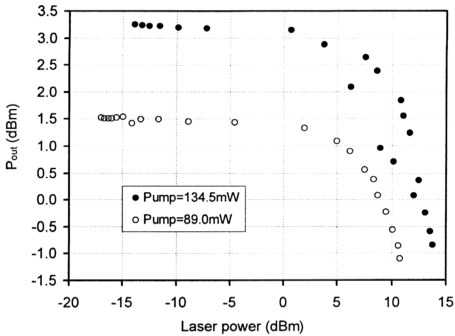


**Fig. 5.27** *Amplified output signal power at $\lambda_{sig}$ = 1550 nm as a function of laser peak power.*

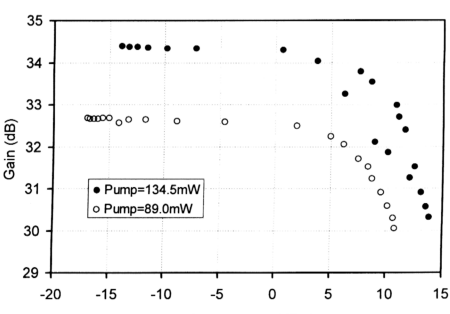


**Fig. 5.28** Signal gain *at $\lambda_{sig}$ = 1550 nm as a function of laser peak power.*

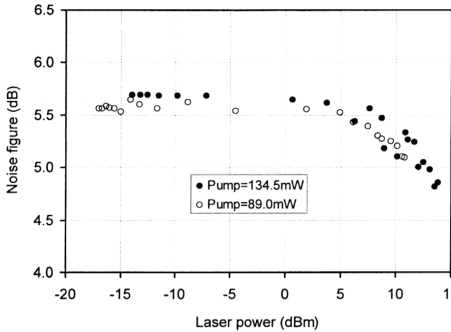


**Fig. 5.29** *Dependence of the noise figure on the laser peak power with the fixed pump powers of $P_p$ = 89 mW and 134.5 mW.*

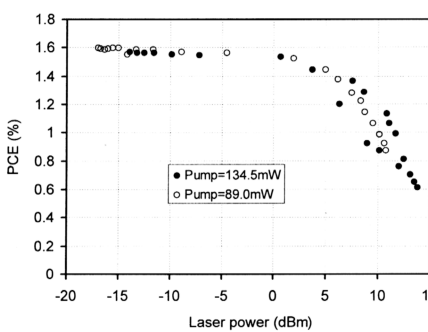


**Fig. 5.30** *Power conversion efficiency as a function of the laser peak power for the pump powers of $P_p$ = 89 mW and 34.5 mW.*

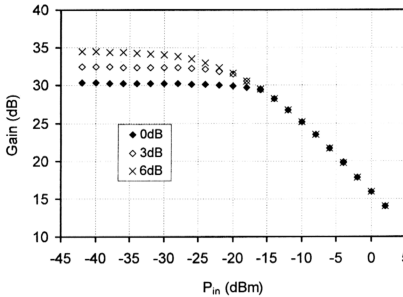


**Fig. 5.31** *Signal gain as a function of the input signal power with the pump fixed at the maximum available power of $P_p$ = 134.5 mW for different attenuation level of 0 dB, 3 dB and 6 dB.*

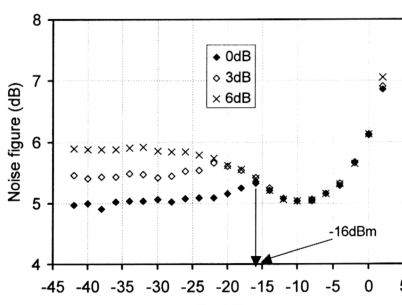


**Fig. 5.32** *Dependence of the noise figure on the input signal power with the pump fixed at the maximum available power of $P_p$ = 134.5 mW for different attenuation level of 0 dB, 3 dB and 6 dB.*

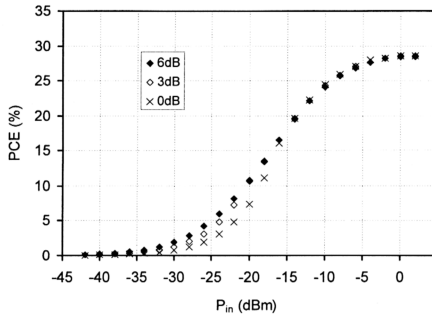


**Fig. 5.33** *Power conversion efficiency as a function of the input signal power.*

## 5.6 EFFECTS OF INPUT SIGNAL ON OSCILLATING LASER

Theoretical and experimental studies of the laser systems subject to an external injection have been intensively studied especially in the case of semiconductor laser [11-13]. In erbium-doped fiber laser (EDFL) systems, some works have been carried out to investigate the frequency control characteristics [14], injection-locking [15-17] and frequency stabilization [16-17]. In the previous work [18], phenomenon of injection-locking has been defined as when the systems are forced to oscillate at the frequency of the injected signal. This can be realized when the injected power is high enough and the signal wavelength is close enough to the slave laser [19]. In our erbium-doped fiber ring laser-amplifier system, the injected signal is been prevented from oscillating due to the existence of the wavelength selective element (i.e. tunable bandpass filter). Therefore, instead of the injection-locking, phenomenon of the laser level suppression is treated as gain-quenching effect by the external injection.

The output spectrums of the EDFL under external injection are shown in Fig. 5.34. The system was pumped at the power of 43.4 mW. With the fixed power of –18.8 dBm, the injected signal was tuned from the wavelength of 1522 nm to 1568 nm. Fig. 5.34(a) shows the output spectrum of the laser without the external injection. The oscillating laser was fixed at $\lambda_{laser}$ = 1550 m for this study. We have defined the laser SNR as the ratio of the laser peak power to the adjacent ASE level monitored from the output port of the coupler as shown in Fig. 5.1. At the given pump power, the laser has a peak power of 3.27 dBm. With an external signal injected at the wavelength of 1540 nm, as shown in Fig. 5.34(b), the oscillating laser has been suppressed to a lower level due to the partially depletion of the population by the injected signal. The signal experiences a gain of 23.6 dB at this wavelength.

The laser SNR as a function of signal detuning is shown in Fig. 5.35. Three different injected signal powers of –23.1 dBm, -20.8 dBm and –18.8 dBm are presented. At a large positive and negative detuning, the oscillating laser is not significantly affected by the injected signal. The thick dashed-line in the figure indicates the laser SNR of 29.6 dB without external injection. Note that there is a markedly reduction in the laser SNR at the negative detuning of 16 nm, corresponding to the wavelength range around 1533 nm in the ASE spectrum, for the injected signal powers of –20.8 dBm and –18.8 dBm. Strong amplification of the injected signal in the region of 1533 nm effectively quenches the gain of the oscillating laser. The laser SNR has been suppressed to 24.0 dB and 26.3 dB for the injected power of –18.8 dBm and –20.8 dBm, respectively. There is no significant variation of laser SNR for the injected power of –23.1 dBm. With the negative detuning of 12 nm, the laser SNR has been restored back to a higher level. This is attributed to the dip at the region around 1540 nm (as shown in Fig.5.34) where the injected signal experiences a

smaller amplification. Consequently, gain quenching effect is less. Further tuning the signal towards the oscillating laser, the laser SNR is found to be continuously reduced. The laser SNR is suppressed to be the lowest at the wavelengths close to zero detuning. However, this is valid only for the case of negative detuning. In the case of positive detuning, the laser SNR continuously decreases although the injected signal is tuned away from the oscillating laser. The minimum laser SNR of 2.4 dB, 5.8 dB and 11.6 dB are achieved for the injected signal power of –18.8 dBm, -20.8 dBm and –23.1 dBm, respectively, at the signal detuning of 8 nm. The lowest laser SNR in this regime can be attributed to the higher signal gain at the region of 1558 nm as compared to the 1550 nm region. At the large positive detuning (> 15 nm), the laser SNR increases owing to the smaller gain quenching effect.

In Fig. 5.36, the injected signal power required to suppress the laser SNR to be just below 10 dB is presented as a function of the signal detuning. Similar to Fig. 5.35, the graph shows an inverse relation with the forward ASE output profile. At large wavelength detuning (> 20 nm), injected signal power of more than –16 dBm is required to suppress the laser SNR to be below 10 dB. However, injected signal power of only –19.5 dBm is enough to suppress the oscillating laser at the negative detuning of 17 nm due to the strong amplification of the signal. With the signal tuned to the low gain regime which is corresponding to the negative detuning of ~12 nm, injected signal power as high as –16.1 dBm is applied. The lowest injected signal power, –22.6 dBm, is achieved at the positive detuning of 8.5 nm. The high gain experiences by the small-injected signal at this wavelength enables it to effectively quench the level of the oscillating laser.

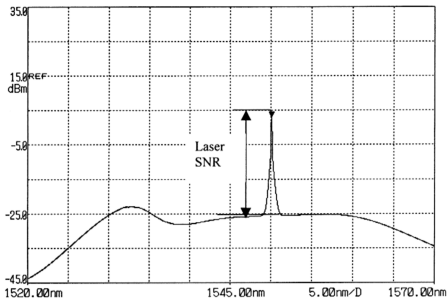


(a)

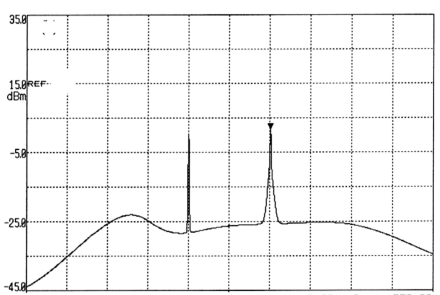


(b)

**Fig. 5.34** *Output spectrums of the EDFL at $P_p$ = 43.4 mW and $P_{in}$ = –18.8 dBm (a) without the external injection. Laser SNR is defined as the ratio of the laser peak power to the adjacent ASE level monitored from the output port of the coupler $C_2$. (b) with external signal injected at the wavelength of 1540 nm.*

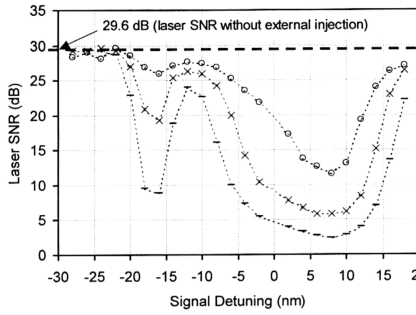


**Fig. 5.35** *Dependence of laser SNR on signal detuning with $P_p$ = 43.4 mW.*
*o: Injected power = -23.1 dBm*
*x: Injected power = -20.8 dBm*
*-: Injected power = -18.8 dBm*

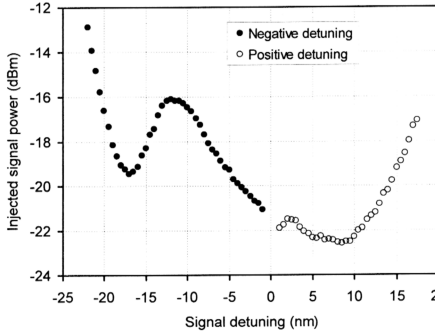


**Fig. 5.36** *Injected signal power as a function of signal detuning with $P_p$ = 43.4 mW*

## 5.7 CONCLUSIONS

Performance of erbium-doped fiber amplifier with optical co-feedback has been demonstrated. Comparison with the counter-feedback scheme and the system without feedback showed that the co-feedback scheme exhibited much lower noise figure in the high pump regime due to the effectiveness of the backward ASE suppression by the oscillating laser in the clock-wise direction. However, the signal gain was found to be degraded by ~1 dB as compared to the counter-feedback system. Laser-induced saturation in the counter-feedback scheme and laser-induced backward ASE suppression at the EDF input end in the co-feedback scheme caused both schemes manifested an opposite behavior in terms of noise figure. Study of the attenuation level in the co-feedback system showed that the performance of the gain-clamped EDFA in terms of signal gain, noise figure and dynamic range were cavity-loss dependent. The oscillating laser of the co-feedback scheme was studied with the existence of the injected signal. The laser SNR was found to be dependent on both injection level and wavelength separation between the oscillating laser and the injected signal.

## REFERENCES

[1] A. E. Siegman, Lasers, University Science Books, CA, 1986.

[2] M. F. Krol, Y. Liu, J. J. Watkins and M. J. Dalley, "Gain Variation in Optically Gain Clamped Erbium Doped Fiber Amplifiers." ECOC'98, pp. 43, 1998; M. F. Krol, Y. Q. Liu, J. J. Watkins and D. W. Lambert, "Dual cavity optical automatic gain control for EDFA," OFC/IOOC '99. Technical Digest , 2, pp. 214 , 1999.

[3] M. Cai, X. Liu, J. Cui, P. Tang, and J. Peng, "Study on noise characteristic of gain-clamped erbium-doped fiber-ring lasing amplifier," IEEE Photonics. Technol. Lett., 9, pp. 1093, 1997.

[4] H. Kawakami, A. Sano and K. Hagimoto, "Gain optimization of an erbium doped fibre for remote pumping system," Electron. Lett., 33, pp. 523, 1997.

[5] R. I. Laming, J. E. Townsend, D. N. Payne, F. Meli, G. Grasso and E. J. Tarbox, "High Power Erbium-Doped Fiber Amplifiers Operating in the Saturated Regime," IEEE Photonics. Technol. Lett., 3, pp. 253, 1991.

[6] R. G. Smart, J. L. Zyskind, J. W. Sulhoff, and D. J. DiGiovanni, "An Investigation of the Noise Figure and Conversion Efficiency of 0.98 μm Pumped Erbium-Doped Fiber Amplifiers Under Saturated Conditions," IEEE Photon. Technol. Lett., 4 pp. 1261, 1992.

[7] Tuan Chin TEYO, Mun Kiat LEONG and Harith AHMAD, "Noise Characteristics of Erbium-Doped Fiber Amplifier with Optical Counter-Feedback," Jpn. J. Appl. Phys. 41, Part 1, No. 5A, pp. 2949, 2002.

[8] T. C. Teyo, M. K. Leong and H. Ahmad, "Noise Characteristics of Erbium-doped Fiber Amplifier With Different Optical Feedback Schemes," Opt. Comm., 207, pp.327, 2002.

[9] E. Desurvire, "Erbiun-doped Fiber Amplifiers – Principles and Applications," John Wiley & Sonc, Inc., 1994.

[10] J. Wilson, "Lasers Principles and Applications" Prentice Hall, 1987.

[11] V. Annovazzi-Lodi, S. Donati, and M. Manna, "Chaos and locking in a semiconductor laser due to external injection," IEEE J. Quantum. Electron., 30 pp. 1537, 1994.

[12] J. Troger, L. Thévenaz, P. A. Nicati and P. A. Robert, "Theory and experiment of a single-mode diode laser subject to external light injection from several lasers," J. Lightwave Technol., 17, pp. 629, 1999.

[13] Y. Matsui, S. Kutsuzawa, S. Arahira, Y. Ogawa, and A. Suzuki, "Bifurcation in 20-GHz gain-switched 1.55-μm MQW lasers and its control by CW injection seeding," IEEE J. Quantum Electron., 34, pp. 1213, 1998.

[14] M. Matsuura and N. Kishi, "Frequency control characteristics of a single-frequency fiber laser with an external light injection," IEEE J. Select. Topics in Quantum Electron., 7, pp. 55, 2001.

[15] J. D. C. Jones and P. Urquhart, "An injection-locked erbium fiber laser," Opt. Comm., 76, pp. 42, 1990.

[16] T. C. Teyo, V. Sinivasagam, M. K. Abdulah and H. Ahmad, "An injection-locked erbium-doped fiber ring laser," Opt. & Laser Technol., 31, pp. 493, 1999.

[17] T. C. Teyo, T. Subramaniam, P. Poopalan and H. Ahmad, "Erbium-doped fiber ring laser subject to an external injection," Proc 2nd East Asian Conf. On Lightwave Systems, Lasers, and Optoelectronics, , pp. 360. 2001

[18] V. Annovazzi-Lodi, A. Sciré, M. Sorel and S. Donati, "Dynamic behavior and locking of a semiconductor laser subjected to external injection, IEEE J. Quantum Electron., 34, pp. 2350, 1998.

[19] P. Even, K. Ait Ameur and G. M. Stéphan, "Modeling of an injected gas laser," Phys. Rev A, 55, pp. 1441, 1997.